

FINITE ELEMENT ANALYSIS OF PORES DESIGN AND TISSUE DIFFERENTIATION IN CEMENTLESS HIP PROSTHESIS

(ECCM –ECFD 2018 CONFERENCE)

HASSAN MEHBOOB¹, FARIS TARLOCHAN¹, SAMI ALKHATIB¹, ALI MEHBOOB²
AND SEUNG HWAN CHANG²

¹Mechanical and Industrial Engineering, Qatar University, Qatar, hassan.mehboob@qu.edu.qa, sa1103668@qu.edu.qa, faris.tarlochan@qu.edu.qa, www.qu.edu.qa

²School of Mechanical Engineering, Chung-Ang University, 221, Heukseok-Dong, Dongjak-Gu, Seoul 156-756, Republic of Korea, alimehboob@cau.ac.kr, phigs4@cau.ac.kr, www.cau.ac.kr

Key words: Hip prosthesis; Pores design; Finite Element Analysis.

Abstract. Cementless hip prostheses are commonly used to repair the femur bones. The primary stability of the hip prosthesis highly dependent on the peri-prosthetic bone ingrowth into the porous structure which is influenced by mechanical and biological environments. 3D finite element models of homogenous and functionally graded porous structures were designed to estimate the bone ingrowth using mechano-regulation algorithm. 200 μm and 800 μm pore spacing for homogenous structures were used, however, for functionally graded structures, the pore spacing was increased and decreased linearly across the length between 200 to 800 μm . Bone ingrowth were simulated using 25 μm micromovements which was determined from macro models. Functionally graded decreasing porous structure showed the highest bone ingrowth 98% with the most uniform tissues distribution.

1 INTRODUCTION

Total hip replacement (THR) is a common procedure to repair the damaged femur bones. Prosthesis made of stainless steel, Cobalt-Chromium (CoCr) and titanium alloy are commonly used to fix the bones [1]. Porous, semi porous, functionally graded materials and composite materials are widely used over a decade to overcome the complications of post-surgery such as aseptic loosening, stress shielding and implant failure etc. [2-4]. These cementless hip prosthesis are generally coated with a porous material to facilitate the bone ingrowth which is fixed proximally in the trabecular bone [5]. This bone ingrowth is influenced by biological and mechanical environments around the hip prosthesis. To control the biomechanical environment, many parameters are involved such prosthesis design, stiffness, pores, beads, interfacial conditions and micromovements [6, 7]. It was reported that micromovements should be less than 100 μm for the successful bone ingrowth, however, $>100 \mu\text{m}$ lead the granulation tissue to the fibrous connective tissue and ultimately failure of prosthesis. Few studies have considered the effects of beads and micromovements on the bone ingrowth. Computer models and simulations are widely in the field of biomechanics. Bone ingrowth is

simulated using various mechano-regulation theories. One of the most efficient mechano-regulation based on the deviatoric strain and fluid flow which is used in our study.

In our study, 3D micromodels of porous structures were constructed in commercially available code ABAQUS 6.17. Homogenous and functionally graded pores spaces were introduced into the microstructures to estimate the bone ingrowth. 25 μm micromovements were generated to check the influence of mechanical environment on tissue differentiation process. A user's subroutine Python was used to program the mechano-regulation algorithm which was employed using ABAQUS. An iterative calculation was made to predict the tissue differentiation for 60 days.

2 MATERIALS AND METHODS

2.1 Finite element macro models

The finite element code ABAQUS was used to create the 3D macro models of femur bone and the prosthesis for the prediction of the bone-prosthesis interfacial micromotions. For simplicity, the femur and the femoral prosthesis were modeled as cylinders with only the diaphyseal section of the bone [8]. The bone model consisted of a cortical and trabecular bone sections of 6.55-mm and 4-mm thickness, respectively. The femoral prosthesis had a diameter of 10 μm which was inserted inside the bone using the interference press fit option in ABAQUS. Loading conditions (axial direction: 2288 N, lateral directions: 862 and 99 N) were applied at the proximal end of the femoral prosthesis representing physiological muscular and weight forces during the stance phase of a gait cycle [9]. The cortical bone was modeled as anisotropic material properties in the cylindrical axis. On the other hand trabecular bone and the femoral stem were modeled as linearly isotropic properties[10]. 8 nodes solid elements C3D8R were used to mesh both the femur bone and the femoral stem models and a coefficient of friction 0.4 was used to mimic the rough contact between the femur and the stem [11]. Maximum micromovements were calculated along the stems which were further used in micromodels.

2.2 Finite element micro models

The micro models of the femur and femoral stem were used to estimate the tissue differentiation process using micromovements of macro models. The micromovements were then used as an input to study the bone ingrowth in porous microstructures. The bone ingrowth is at an optimal level when the pore size range is between 200-800 μm . Hence, porous microstructures with fixed representative volume element (RVE) were created with two levels of pore sizes 200 and 800 μm . The bead diameter of the microstructures was fixed (500 μm) because it has insignificant effect on bone ingrowth relative to the effect of the pore size. Four configurations of pore spacing were considered; homogeneous configuration (200 and 800 μm), and functionally graded pores configuration (functionally graded pores increasing FGPI and functionally graded pores decreasing FGPD). The design space, including the porosity and the pore sizes, of both the homogeneous and FGP configurations is depicted in **Fig. 1**. The FGP configuration was modeled as FGP increasing (FGPI) where the pore sizes were increased linearly in the axial direction and FGP decreasing (FGPD) where the pore sized where decreased linearly in the axial direction as illustrated in **Fig. 1**. The pore

spacings were varied along the axial direction (z-axis), while they were fixed at 200 μm in the x-axis. The beads were fitted in the bone using an interference press fit of 5 μm . Callus was inserted in the gap between the femur and the femoral stems, and a friction coefficient of 0.4 was introduced to account for the contact between the beads and the callus. The beads material was modelled as isotropic titanium alloy properties. 8 nodes solid poroelastic elements were used to mesh the bone and the callus, and 8 nodes solid elements were used to mesh the beads and the femoral stem.

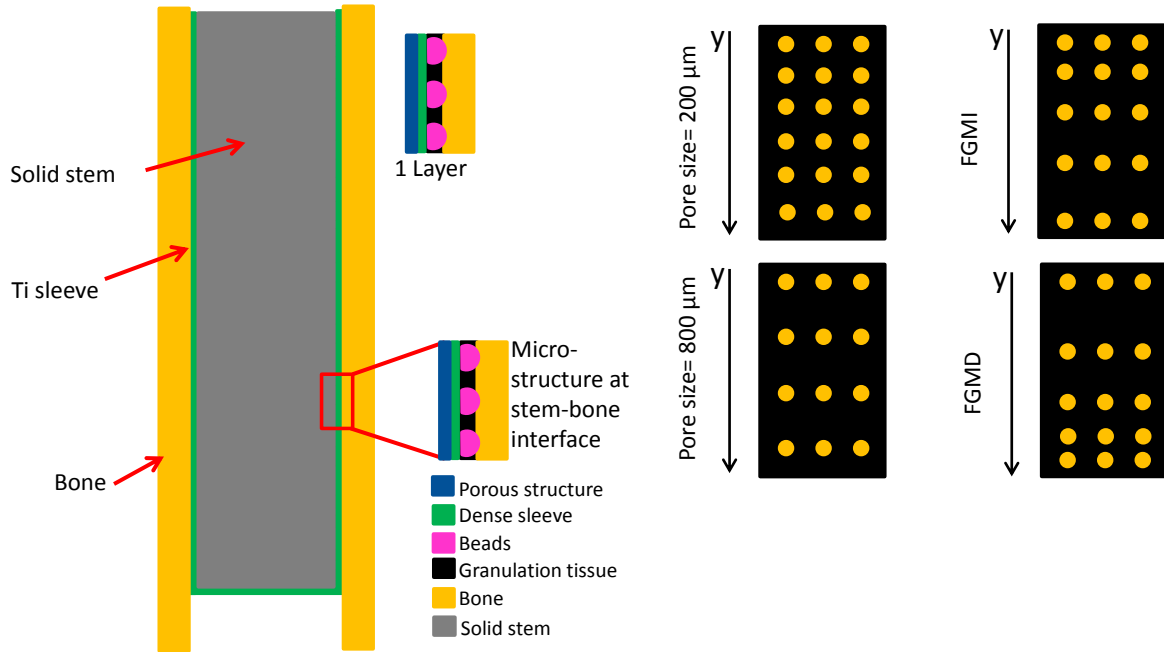


Fig. 1 Finite element models of macro and micro models

2.3 Loading and boundary conditions

To mimic the interference fit of bone and prosthesis, a pressure of 0.5 MPa was applied on the prosthesis and bone was fixed on opposite direction. A load was applied to the prosthesis on the axial direction to generate the micromovements. Loads were applied to generate 25 μm micromovements initially.

2.4 Mechano-regulation theory

Compute models were coupled with mechano-regulation algorithm to predict the bone ingrowth. A mechano-regulation model with deviatoric strain and fluid flow was utilized to estimate the tissue differentiation in micro models. Iterative calculations were performed to update the material properties of tissue phenotype using Python code as shown in **Fig. 2**.

3 RESULTS AND DISCUSSION

Micromovements between bone and prosthesis were determined as 25 μm which were applied to the micromodels. Spatial and temporal tissue differentiation was estimated.

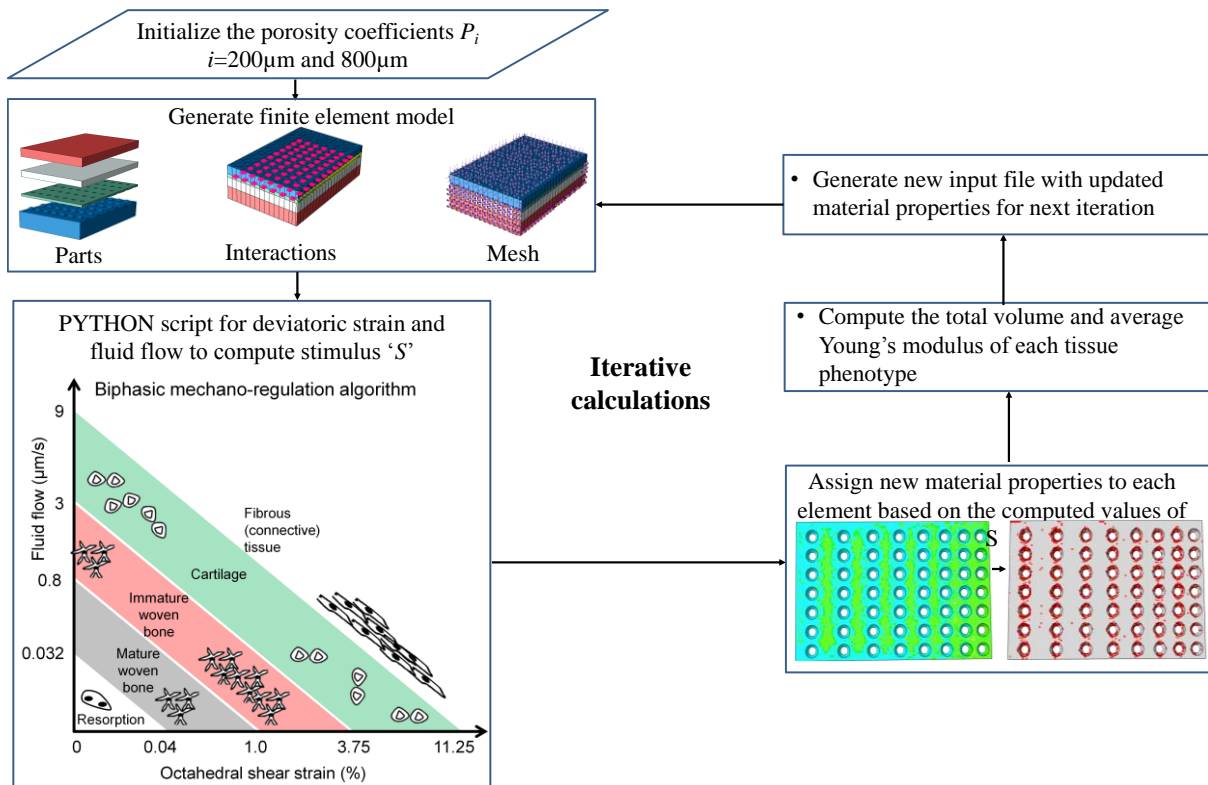


Fig. 2 Mechano-regulation algorithm and iterative calculation to predict the tissue differentiation process

3.1 Spatial distribution of tissue phenotypes

Spatial distributions of tissue phenotypes was predicted in the case of 200 μm , 800 μm , FGPI and FGPD micro models as shown in **Fig. 3**. It was seen that 200 μm pore space gave better tissue maturation as compared to 800 μm pore space. Stimulus was not enough to stimulate the soft tissue and differentiate them to the next levels. Therefore, a combination of granulation and fibrous tissues was present in the first iteration. However, in iteration 60, the most of the tissues were developed to the mature bone in the case of 200 μm pore space. But in the case of 800 μm pore space, tissues were still in the immature bone phase to insufficient stimulus. Similarly, FGPI pore space gave poor results as compared to the FGPD due the fact that stimulus values decrease along the length of the prosthesis thus smaller pore spaces still gave better tissue differentiations.

3.2 Percentage of tissue development

A quantitative analysis was performed to estimate the percentage of tissue phenotypes developed in all the cases as shown in **Fig. 4**. The granulation tissues were differentiated into the fibrous tissues, cartilage and immature bone within 10 iterations. However, it was observed that the transition phase from intermediate bone to the mature bone development was around 20th iteration. The intermediate and mature bone formation was least in the case of 800 μm pore space. The maximum intermediate and mature bone formation was seen in FGPI pore space.

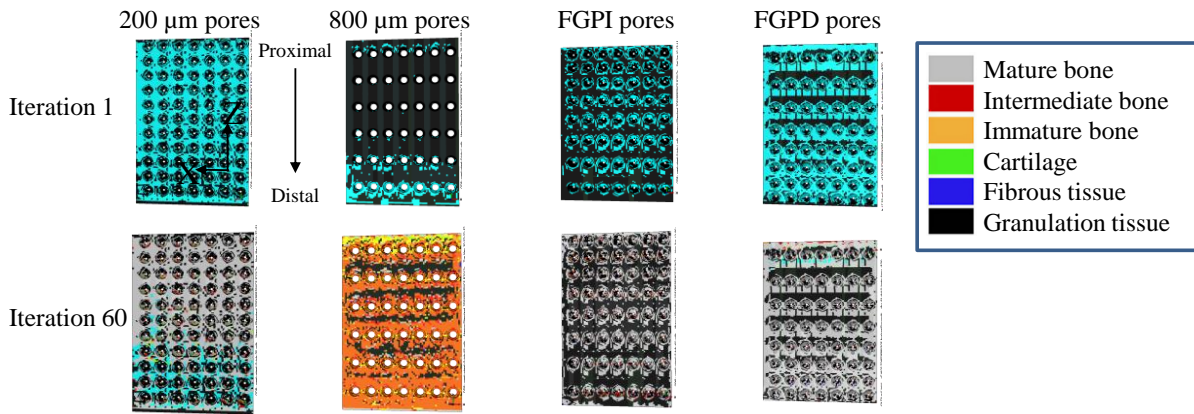


Fig. 3 Spatial distribution of tissue phenotypes in homogenous and functionally graded porous structures

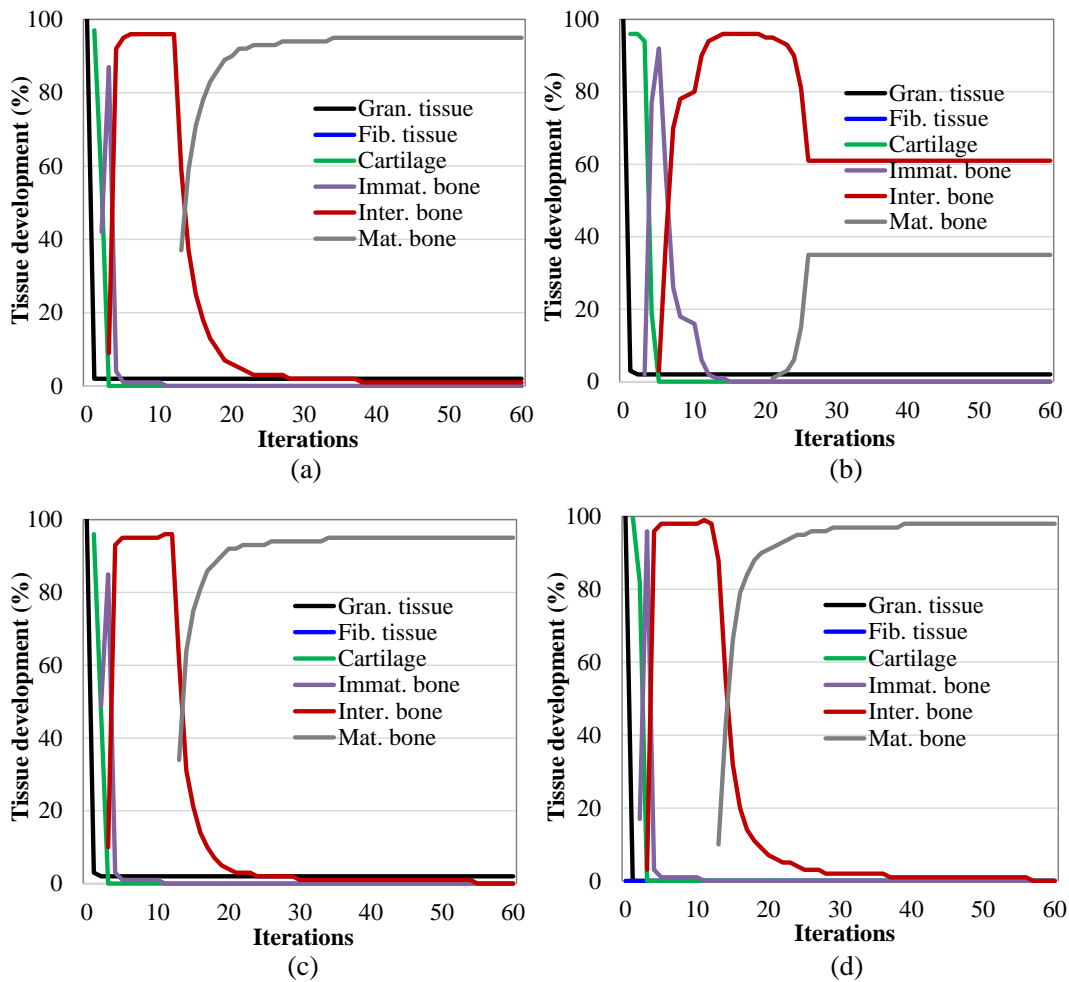


Fig. 4 Tissue differentiation process using finite element analyses; (a) 200 μm homogenous pore spaces, (b) 800 μm homogenous pore spaces, (c) functionally graded increasing pore spaces (FGPI) and (d) functionally graded decreasing pore spaces (FGPD)

4. CONCLUSIONS

- Smaller pore space (200 μ m) gave the higher tissue differentiation and maturation, on the other hand, in the case of 800 μ m compromised with the volume of callus development.
- Functionally graded pore decreasing enhanced the homogeneity of tissue distribution within the callus and the percentage of tissue development to the bones.

ACKNOWLEDGEMENT

This paper was made possible by NPRP grant# NPRP 8-876-2-375 from the Qatar National Research Fund (a member of Qatar Foundation). The findings achieved herein are solely the responsibility of the authors.

REFERENCES

1. Chen QZ, Thouas GA. Metallic implant biomaterials. *Mat Sci Eng R*. 2015;87:1-57.
2. Arabnejad S, Johnston B, Tanzer M, Pasini D. Fully porous 3D printed titanium femoral stem to reduce stress-shielding following total hip arthroplasty. *J Orthop Res*. 2016.
3. Ataollahi Oshkour A, Pramanik S, Mehrali M, Yau YH, Tarlochan F, Abu Osman NA. Mechanical and physical behavior of newly developed functionally graded materials and composites of stainless steel 316L with calcium silicate and hydroxyapatite. *J Mech Behav Biomed Mater*. 2015;49:321-31.
4. Simoneau C, Terriault P, Jette B, Dumas M, Brailovski V. Development of a porous metallic femoral stem: Design, manufacturing, simulation and mechanical testing. *Mater Design*. 2017;114:546-56.
5. Mukherjee K, Gupta S. Bone ingrowth around porous-coated acetabular implant: a three-dimensional finite element study using mechanoregulatory algorithm. *Biomech Model Mechan*. 2016;15:389-403.
6. Liu XY, Niebur GL. Bone ingrowth into a porous coated implant predicted by a mechano-regulatory tissue differentiation algorithm. *Biomech Model Mechan*. 2008;7:335-44.
7. Viceconti M, Pancanti A, Dotti M, Traina F, Cristofolini L. Effect of the initial implant fitting on the predicted secondary stability of a cementless stem. *Med Biol Eng Comput*. 2004;42:222-9.
8. Gross S, Abel EW. A finite element analysis of hollow stemmed hip prostheses as a means of reducing stress shielding of the femur. *J Biomech*. 2001;34:995-1003.
9. Sridhar I, Adie PP, Ghista DN. Optimal design of customised hip prosthesis using fiber reinforced polymer composites. *Mater Design*. 2010;31:2767-75.
10. Donahue TL, Hull ML, Rashid MM, Jacobs CR. A finite element model of the human knee joint for the study of tibio-femoral contact. *J Biomech Eng*. 2002;124:273-80.
11. Kadir MRA, Kamsah N, Mohlisun N. Interface Micromotion of Cementless Hip Arthroplasty: Collared vs Non-collared Stems. *Ifmbe Proc*. 2008;21:428-+.